

Penalty Method for Inversion-Free Deep Bilevel Optimization

Akshay Mehra¹ Jihun Hamm¹

Abstract

Bilevel optimization problems are at the center of several important machine learning problems such as hyperparameter tuning, data denoising, meta- and few-shot learning, data poisoning. Different from simultaneous or multi-objective optimization, bilevel optimization requires computing the inverse of the Hessian of the lower-level cost function to obtain the exact descent direction for the upper-level cost. In this paper, we propose a new method for solving deep bilevel optimization problems using the penalty function which avoids computing the inverse. We prove convergence of our method under mild conditions and show that it computes the exact hypergradient asymptotically. Small space and time complexity of our method enables us to solve large-scale bilevel problems involving deep neural networks with several million parameters. We present results of our method for data denoising on MNIST/CIFAR10/SVHN datasets, for few-shot learning on Omniglot/Mini-Imagenet datasets and for training-data poisoning on MNIST/Imagenet datasets. In all experiments, our method outperforms or is comparable to previously proposed methods both in terms of accuracy and run-time.

1. Introduction

Solving a bilevel optimization problem is crucial for the fields of study which involve a competition between two parties or two objectives. Particularly, a bilevel problem arises, if one party makes its choice first affecting the optimal choice for the second party, also known as the Stackelberg model, dating back to 1930’s [von Stackelberg, 2010]. The general form of a bilevel optimization problem is

$$\min_u f(u, v), \quad \text{s.t.} \quad v = \arg \min_v g(u, v). \quad (1)$$

¹Department of Computer Science, Tulane University. Correspondence to: Akshay Mehra <amehra@tulane.edu>, Jihun Hamm <jhamm3@tulane.edu>.

A bilevel problem with constraints is of the form $\min_{u \in \mathcal{U}} f(u, v)$, s.t. $v = \arg \min_{v \in \mathcal{V}(u)} g(u, v)$, where the lower-level constraint set $\mathcal{V}(u)$ can depend on u . However, we focus on unconstrained problems in this paper. The ‘upper-level’ problem $\min_u f(u, v)$ is a usual minimization problem except that v is constrained to be the solution to the ‘lower-level’ problem $\min_v g(u, v)$ which is dependent on u (see [Bard, 2013] for a review of bilevel optimization). Bilevel optimizations also appears in many important machine learning problems. For example, gradient-based hyperparameter tuning [Domke, 2012; Maclaurin et al., 2015; Luketina et al., 2016; Pedregosa, 2016; Franceschi et al., 2017; 2018], data denoising by importance learning [Liu & Tao, 2016; Yu et al., 2017; Ren et al., 2018], few-shot learning [Ravi & Larochelle, 2017; Santoro et al., 2016; Vinyals et al., 2016; Franceschi et al., 2017; Mishra et al., 2017; Snell et al., 2017; Franceschi et al., 2018; Rajeswaran et al., 2019], and training-data poisoning [Mei & Zhu, 2015; Muñoz-González et al., 2017; Koh & Liang, 2017; Shafahi et al., 2018]. We explain each of these problems and their bilevel formulations below.

Gradient-based hyperparameter tuning. Finding hyperparameters is an indispensable step in any machine learning problem. Grid search is a popular way of finding the optimal hyperparameters, if the domain of the hyperparameters is a predetermined discrete set or a range. However, when losses are differentiable functions of the hyperparameter(s), we can find optimal hyperparameter values by solving a continuous bilevel optimization. Let u and w denote hyperparameter(s) and parameter(s) for a class of learning algorithms and $h(x; u, w)$ be the hypothesis. Then $L_{\text{val}}(u, w) := \frac{1}{N_{\text{val}}} \sum_{(x_i, y_i) \in \mathcal{D}_{\text{val}}} l(h(x_i; u, w), y_i)$ is the validation loss, and $L_{\text{train}}(u, w)$ is the training loss, defined similarly. The best hyperparameter(s) u is then the solution to the following problem

$$\min_u L_{\text{val}}(u, w) \quad \text{s.t.} \quad w = \arg \min_w L_{\text{train}}(u, w). \quad (2)$$

Thus, we find the best model parameters w for each choice of the hyperparameter u , and select that value for the hyperparameter u which incurs the smallest validation loss.

Data denoising by importance learning. A common assumption of learning is that the training examples are i.i.d. samples from the same distribution as the test data. However, if training and testing distributions are not

identical or if the training examples have been corrupted by noise or modified by adversaries, this assumption is violated. In such cases, re-weighting the importance of each training example, before training, can help reduce the discrepancy between the two distributions. For example, one can up-weight the importance of the examples from the same distribution and down-weight the importance of the rest. Finding the correct weight for each training example can be formulated as a bilevel optimization. Consider u to be the vector of non-negative importance values for each training example $u = [u_1, \dots, u_N]^T$ where N is the number of training examples, and w are the parameter(s) of a classifier $h(x; w)$. Then the weighted training error is $L_{w, \text{train}}(u, w) := \frac{1}{\sum_i u_i} \sum_{(x_i, y_i) \in \mathcal{D}_{\text{train}}} u_i l(h(x_i; w), y_i)$. Assuming we have a small number of examples, from the same distribution as the test examples (validation examples) the importance learning problem is:

$$\min_u L_{\text{val}}(u, w) \text{ s.t. } w = \arg \min_w L_{w, \text{train}}(u, w). \quad (3)$$

Hence, the importance of each training example (vector u) is selected such that the minimizer w of the weighted training loss in the lower level also minimizes the validation loss in the upper-level. The final importance values can help to identify good points from the noisy training set and the classifier w obtained after solving this optimization will have superior performance compared to the model trained on the noisy data.

Meta-learning. A standard learning problem involves finding the best model from the class of hypotheses for a given task (i.e., data distribution). In contrast, meta-learning is a problem of learning a prior on the hypothesis classes (a.k.a. inductive bias) for a given set of tasks. Few-shot learning is an example of meta-learning, where a learner is trained on several related tasks, during the meta-training phase, so that it can generalize well to unseen (but related) tasks with just few examples, during the meta-testing phase. An effective approach to the few-shot learning problem is to learn a common representation for various tasks and train task specific classifiers on top of this representation. Let T be the map that takes raw features to a common representation $T: \mathcal{X} \rightarrow \mathbb{R}^d$ for all tasks and h_i be the classifier for the i -th task, $i \in \{1, \dots, M\}$ where M is the total number of tasks for training. The goal of few-shot learning is to learn both the representation map $T(\cdot; u)$ parameterized by u and the set of classifiers $\{h_1, \dots, h_M\}$ parameterized by $w = \{w_1, \dots, w_M\}$. Let $L_{\text{val}}(u, w_i) := \frac{1}{N_{\text{val}}} \sum_{(x_i, y_i) \in \mathcal{D}_{\text{val}}} l(h_i(T(x_i; u); w_i), y_i)$ be the validation loss of task i and $L_{\text{train}}(u, w_i)$ be the training loss defined similarly, then the bilevel problem for few-shot learning is

$$\begin{aligned} \min_u \sum_i L_{\text{val}}(u, w_i) \\ \text{s.t. } w_i = \arg \min_{w_i} L_{\text{train}}(u, w_i), i = 1, \dots, M. \end{aligned} \quad (4)$$

For evaluation of the learned representation, during the meta-test phase, the representation $T(\cdot; u)$ is kept fixed and only the classifiers for the new tasks $\{h_1, \dots, h_N'\}$ are trained i.e. $\min_{w_i'} L_{\text{test}}(u, w_i') \quad i = 1, \dots, N$ where N is the total number of tasks for testing.

Training-data poisoning. Recently, machine learning models were shown to be vulnerable to train-time attacks. Different from the test time attacks, here adversary modifies the training data so that the model learned from altered training data performs poorly/differently as compared to the model learned from clean data. The most popular train-time attack method augments the original training data $X = \{x_1, \dots, x_N\}$ with one or more ‘poisoned’ examples $u = \{u_1, \dots, u_M\}$ i.e., $X' = X \cup u$, assigning them arbitrary labels, to create the poisoned dataset with $L_{\text{poison}}(u, w) := \frac{1}{N} \sum_{(x_i, y_i) \in X' \times Y} l(h(x_i; u, w), y_i)$ being the loss on the poisoned training data. The problem of finding poisoning points, that when added to the clean training data hurt the performance of the model trained on it can be formulated as

$$\min_u -L_{\text{val}}(u, w) \text{ s.t. } w = \arg \min_w L_{\text{poison}}(u, w), \quad (5)$$

where the minus sign in the upper-level is used to maximize the validation loss. This is the formulation for untargeted attacks. For targeted attacks, the upper-level must minimize the validation loss with respect to the intended target labels of the attacker. Another variant of the poisoning attack, only influences the prediction of a single predetermined example. The upper-level cost for such an attack is the loss over this particular example (see Eq. (10) in the Appendix E.4.1).

Challenges of deep bilevel optimization. General bilevel optimization problems cannot be solved using simultaneous optimization of the upper- and lower-level costs. Moreover, exact solution to a bilevel optimization is known to be NP-hard even for linear cost functions [Bard, 1991]. To add to this, recent deep learning models, with millions of variables, make it infeasible to use sophisticated methods beyond the first-order methods. But, for bilevel problems, even the first-order methods are difficult to apply since they require computation of the inverse Hessian–gradient product to get the exact hypergradient (see Sec. 2.1). Since direct inversion of the Hessian is impractical even for moderate-sized problems, many approaches have been proposed to approximate the exact hypergradient including forward/reverse-mode differentiation [Maclaurin et al., 2015; Franceschi et al., 2017; Shaban et al., 2018] and approximate inversion by solving a linear system of equations [Domke, 2012; Pedregosa, 2016; Rajeswaran et al., 2019]. But, still there is a big room for improvement in these existing approaches in terms of their space and time complexities and their practical performance.

Contributions. We propose a penalty function-based algorithm (Alg. 1) for solving large-scale unconstrained

bilevel optimization problems. We prove convergence of the method under mild conditions (Theorem 2) and show that it computes the exact hypergradient asymptotically (Lemma 3). We present complexity analysis of the algorithm showing that it has linear time and constant space complexity (Table 1), making our method superior to forward-mode and reverse-mode differentiation and similar to the approximate inversion based method. Small space and time complexity of our approach enables us to solve large-scale bilevel problems involving deep neural networks (Table 7 in Appendix E). We apply our method (Penalty) to solve various machine learning problems like data denoising, few-shot learning, and training-data poisoning. Penalty performs competitively to the state-of-the-art methods on simpler problems (with convex lower-level cost) and significantly outperforms other methods on complex problems (with non-convex lower-level cost), both in terms of accuracy (Sec. 3) and run-time (Table 2 and Fig. 4 in Appendix D) showing that it is an effective solver for various bilevel problems.

The remainder of the paper is organized as follows. We present and analyze the main algorithm in Sec. 2, perform comprehensive experiments in Sec. 3, and conclude the paper in Sec. 4. Due to space limitation, proofs, experimental settings and additional results are presented in the appendix. All codes are uploaded to [Github](#).

2. Inversion-Free Penalty Method

Throughout the paper we have assumed that upper- and lower-level costs f and g are twice continuously differentiable in both u and v . We use $\nabla_u f$ and $\nabla_v f$ to denote gradient vectors, $\nabla_{uv}^2 f$ for the matrix $\left[\frac{\partial^2 f}{\partial u_i \partial v_j} \right]$, and $\nabla_{vv}^2 f$ for the Hessian matrix $\left[\frac{\partial^2 f}{\partial v_i \partial v_j} \right]$. Additionally, following previous works we have assumed that the lower-level solution $v^*(u) := \arg \min_v g(u, v)$ is unique for all u and that $\nabla_{vv}^2 g$ is invertible everywhere. Later in this section we discuss relaxation for some of these assumptions.

2.1. Hypergradient for bilevel optimization

Assuming we can express the solution to the lower-level problem $v^*(u) := \arg \min_v g(u, v)$ explicitly, we can write the bilevel problem as an equivalent single-level problem $\min_u f(u, v^*(u))$. We can use gradient-based approach on this single-level problem and compute the total derivative $\frac{df}{du}(u, v^*(u))$, called the hypergradient, in previous approaches. Using the chain rule, the total derivative is

$$\frac{df}{du} = \nabla_u f + \frac{dv}{du} \cdot \nabla_v f, \text{ at } (u, v^*(u)) \quad (6)$$

In reality, $v^*(u)$ can be written explicitly only for trivial problems, but we can still compute $\frac{dv}{du}$ using the implicit function theorem. Since $\nabla_v g = 0$ at

$v = v^*(u)$, we get $du \cdot \nabla_{uv}^2 g + dv \cdot \nabla_{vv}^2 g = 0$ and consequently $\frac{dv}{du} = -\nabla_{uv}^2 g (\nabla_{vv}^2 g)^{-1}$. Thus, the hypergradient from Eq. (6) is as follows

$$\frac{df}{du} = \nabla_u f + \frac{dv}{du} \nabla_v f = \nabla_u f - \nabla_{uv}^2 g (\nabla_{vv}^2 g)^{-1} \nabla_v f \quad (7)$$

Existing approaches [Domke, 2012; Maclaurin et al., 2015; Pedregosa, 2016; Franceschi et al., 2017; Shaban et al., 2018; Rajeswaran et al., 2019] can be viewed as implicit methods of approximating the hypergradient, with distinct trade-offs in efficiency and complexity.

2.2. Penalty function approach

A bilevel problem can be considered as a constrained optimization problem since the lower-level optimality $v = \arg \min_v g(u, v)$ is a constraint, in addition to any other constraint in the upper- and the lower-level problems. In this work, we focus on unconstrained bilevel problems i.e. those without any additional constraints on the upper- and lower-level problems. For solving such bilevel problems, the lower-level problem is often replaced by its necessary condition for optimality, resulting in the following problem:

$$\min_{u, v} f(u, v), \quad \text{s.t.} \quad \nabla_v g(u, v) = 0 \quad (8)$$

For general bilevel problems, Eq. (8) and Eq. (1) are not the same [Dempe & Dutta, 2012]. But, with lower-level cost g being convex in v for each u and the assumption that the lower-level solution is unique for each u , Eq. (8) is equivalent to Eq. (1).

We now describe the penalty function approach for solving bilevel optimization. The penalty function method is a well-known approach for solving constrained optimization problems (see [Bertsekas, 1997] for a review) and has been previously applied for solving bilevel problems. However, it was analyzed under strict assumptions and only high-level descriptions of the algorithm were presented before [Aiyoshi & Shimizu, 1984; Ishizuka & Aiyoshi, 1992]. The penalty function $\tilde{f}(u, v; \gamma) := f(u, v) + \frac{\gamma}{2} \|\nabla_v g(u, v)\|^2$, optimizes the original cost f plus a quadratic penalty term (which penalizes the violation of the necessary conditions for lower-level optimality) in Eq. (8). Let (\hat{u}_k, \hat{v}_k) be the minimum of the penalty function \tilde{f} for a given γ_k :

$$(\hat{u}_k, \hat{v}_k) := \arg \min_{u, v} f(u, v) + \frac{\gamma_k}{2} \|\nabla_v g(u, v)\|^2 \quad (9)$$

Then the following convergence result is known.

Theorem 1 (Theorem 8.3.1 of [Bard, 2013]). *Assume f and g are convex in v for any fixed u . Let $\{\gamma_k\}$ be any positive ($\gamma_k > 0$) and divergent ($\gamma_k \rightarrow \infty$) sequence. If $\{(\hat{u}_k, \hat{v}_k)\}$ is the corresponding sequence of optimal solutions of the penalty function Eq. (9), then the sequence $\{(\hat{u}_k, \hat{v}_k)\}$ has limit points any one of which is a solution of Eq. (1).*

Even though this is a strong result, it's not very practical, since the minimum (\hat{u}_k, \hat{v}_k) needs to be computed exactly for each γ_k , $k = 1, 2, \dots$, and moreover f and g need to be convex in v for any u . In our approach, we allow ϵ_k -optimal solutions of Eq. (9) and show convergence to a KKT point of Eq. (8) without requiring convexity.

Theorem 2. Suppose $\{\epsilon_k\}$ is a positive ($\epsilon_k > 0$) and convergent ($\epsilon_k \rightarrow 0$) sequence, and $\{\gamma_k\}$ is a positive ($\gamma_k > 0$), non-decreasing ($\gamma_1 \leq \gamma_2 \leq \dots$), and divergent ($\gamma_k \rightarrow \infty$) sequence. Let $\{(u_k, v_k)\}$ be the sequence of approximate solutions to Eq. (9) with tolerance $(\nabla_u \tilde{f}(u_k, v_k))^2 + (\nabla_v \tilde{f}(u_k, v_k))^2 \leq \epsilon_k^2$ for all $k = 0, 1, \dots$. Then any limit point of $\{(u_k, v_k)\}$ satisfies the KKT conditions of the problem in Eq. (8).

Alg. 1 describes our method in which we minimize the penalty function in Eq. (9), alternatively over v and u . It is essential to note that our method solves a single-level penalty function, Eq. (9), and does not need any intermediate step to compute the approximate hypergradient, unlike other methods which first approximate the solution to the lower-level problem of Eq. (1) and then use an intermediate step (solving a linear system or using reverse/forward mode differentiation) to compute the approximate hypergradient. Lemma 3 (below) shows when the approximate gradient direction $\nabla_u \tilde{f}$, computed from Alg. 1 becomes the exact hypergradient Eq. (7) for bilevel problems.

Lemma 3. Given u , let \hat{v} be $\hat{v} := \arg \min_v \tilde{f}(u, v; \gamma)$ from Eq. (9). Then, $\nabla_u \tilde{f}(u, \hat{v}; \gamma) = \frac{df}{du}(u, \hat{v})$.

Thus if we find the minimizer \hat{v} of the penalty function for given u and γ , Alg. 1 computes the exact hypergradient Eq. (7) at (u, \hat{v}) . Furthermore, under the conditions of Theorem 1, $\hat{v}(u) \rightarrow v^*(u)$ as $\gamma \rightarrow \infty$ and we get the exact hypergradient asymptotically.

Comparison with other methods. Many methods have been proposed previously to solve bilevel optimization problems appearing in machine learning, including forward/reverse-mode differentiation (FMD/RMD) [Maclaurin et al., 2015; Franceschi et al., 2017; Shaban et al., 2018] and approximate hypergradient computation by solving a linear system (ApproxGrad) [Domke, 2012; Pedregosa, 2016; Rajeswaran et al., 2019]. For completeness, we have described these methods briefly in Appendix B. We show the trade-offs of these methods for computing the hypergradient in Table 1. We see that as T (total number of v -updates per one hypergradient computation) increases, FMD and RMD become impractical due to $O(UVT)$ time complexity and $O(U + VT)$ space complexity, respectively, whereas ApproxGrad and Penalty, have the same linear time complexity and constant space complexity, which is a big advantage over FMD and RMD. However, complexity analysis does not show the quality of hypergradient approximation of each method. In Sec. 3.1 we show empirically that the

Algorithm 1 Penalty method for bilevel optimization

Input: $K, T, \{\sigma_k\}, \{\rho_{k,t}\}, \gamma_0, \epsilon_0, c_\gamma (=1.1), c_\epsilon (=0.9)$

Output: (u_K, v_T)

Initialize u_0, v_0 randomly

Begin

for $k = 0, \dots, K-1$ **do**

while $\|\nabla_u \tilde{f}\|^2 + \|\nabla_v \tilde{f}\|^2 > \epsilon_k^2$ **do**

for $t = 0, \dots, T-1$ **do**

v -update: $v_{t+1} \leftarrow v_t - \rho_{k,t} \nabla_v \tilde{f}$ (from Eq. (9))

end for

u -update: $u_{k+1} \leftarrow u_k - \sigma_k \nabla_u \tilde{f}$ (from Eq. (9))

end while

$\gamma_{k+1} \leftarrow c_\gamma \gamma_k, \epsilon_{k+1} \leftarrow c_\epsilon \epsilon_k$

end for

proposed penalty method has better convergence properties than all the other methods with synthetic examples and since ApproxGrad and Penalty have the same complexities we compare them on real data and show that Penalty is superior or comparable to ApproxGrad in performance and time.

Improvements. A caveat to these theoretical guarantees is that some of the assumptions made for analysis may not be satisfied in practice. Here we discuss simple techniques to address these problems and improve Alg. 1 further. The first problem is related to non-convexity of the lower-level cost g , creating the problem that the local minimum of $\|\nabla_v g\|$ can be either a minimum or a maximum of g . To address this we modify the v -update for Eq. (9) by adding a ‘regularization’ term $\lambda_k g$ to the cost. Thus, the v -update becomes $\min_v [f + \frac{\gamma_k}{2} \|\nabla_v g\|^2 + \lambda_k g]$. This only affects the optimization in the beginning; as $\lambda_k \rightarrow 0$ the final solution remains unaffected with or without regularization. The second problem is that the tolerance $\nabla_{(u,v)} \tilde{f}(u_k, v_k; \gamma_k) \leq \epsilon_k$ may not be satisfied in a limited time and the optimization may terminate before γ_k becomes large enough. A cure to this is the method of multipliers and augmented Lagrangian [Bertsekas, 1976] which allows the penalty method to find a solution with a finite γ_k . Thus we add the term $\nabla_v g^T \nu$ to the penalty function (Eq. (9)) to get $\min_{u,v} [f + \frac{\gamma_k}{2} \|\nabla_v g\|^2 + \nabla_v g^T \nu]$ and use the method of multiplier to update ν as $\nu \leftarrow \nu + \gamma \nabla_v g$. In summary, we use the following update rules in the paper.

$$\begin{aligned} u_{k+1} &\leftarrow u_k - \rho \nabla_u \left[f + \frac{\gamma_k}{2} \|\nabla_v g\|^2 + \nabla_v g^T \nu_k \right] \\ v_{k+1} &\leftarrow v_k - \sigma \nabla_v \left[f + \frac{\gamma_k}{2} \|\nabla_v g\|^2 + \nabla_v g^T \nu_k + \lambda_k g \right] \\ \nu_{k+1} &\leftarrow \nu_k + \gamma_k \nabla_v g. \end{aligned}$$

These changes are helpful in theory but were only moderately better than original versions empirically (Appendix C).

Table 1. Complexity analysis of various bilevel methods (Appendix B). U is the size of u , V is the size of v , and T is the number of v -updates per one hypergradient computation. P , p and q are variables of size $U \times V$, $U \times 1$, and $V \times 1$ used to compute the hypergradient. We use gradient descent as the process for FMD and RMD. Hessian-vector product has $O(V)$ complexity [Pearlmutter, 1994].

Method	v -update	Intermediate updates	Time	Space
FMD	$v \leftarrow v - \rho \nabla_v g$	$P \leftarrow P(I - \rho \nabla_{vv}^2 g) - \rho \nabla_{uv}^2 g$	$O(UVT)$	$O(UV)$
RMD	$v \leftarrow v - \rho \nabla_v g$	$p \leftarrow p - \rho \nabla_{uv}^2 g \cdot q$ $q \leftarrow q - \rho \nabla_{vv}^2 g \cdot q$	$O(VT)$	$O(U + VT)$
ApproxGrad	$v \leftarrow v - \rho \nabla_v g$	$q \leftarrow q - \rho \nabla_{vv}^2 g [\nabla_{vv}^2 g \cdot q - \nabla_v f]$	$O(VT)$	$O(U+V)$
Penalty	$v \leftarrow v - \rho [\nabla_v f + \gamma \nabla_{vv}^2 g \nabla_v g]$	Not required	$O(VT)$	$O(U+V)$

3. Experiments

In this section, we evaluate the performance of the proposed penalty method (Penalty) on various machine learning problems discussed in the introduction. We compare Penalty against both bilevel and non-bilevel solutions to these problems previously reported in the literature.

3.1. Synthetic examples

Here we compare Penalty, gradient descent (GD), reverse-mode differentiation (RMD), and approximate hypergradient method (ApproxGrad) on synthetic examples. We omit the comparison with forward-mode differentiation (FMD) because of its impractical time complexity for larger problems. GD refers to the alternating minimization: $u \leftarrow u - \rho \nabla_u f$, $v \leftarrow v - \sigma \nabla_v g$. For RMD, we used the version with gradient descent as the lower-level process. For all ApproxGrad experiments, we used Adam for the updates. We found that Adam solves the linear system just as effectively as conjugate gradient descent (CG) given enough number of iterations and can take advantage of a GPU making it feasible to run more iterations in the same time as taken by CG. Using simple quadratic surfaces for f and g , we compare all the algorithms by observing their convergence as a function of the number of upper-level iterations by varying the number of lower-level updates (T), for computing the hypergradient update. We measure the convergence of these methods using the Euclidean distance of the current iterate (u, v) from the closest optimal solution (u^*, v^*) . Since the synthetic examples are not learning problems, we can only measure the distance of the iterates to an optimal solution $\|(u, v) - (u^*, v^*)\|_2^2$. Fig. 1 shows the performance of two 10-dimensional examples described in the caption (see Appendix E.1). As one would expect, increasing the number T of v -updates makes all the algorithms better since doing more lower-level iterations makes the hypergradient estimation more accurate (Eq. (7)) but it also increases the run time of the methods. However, even for these examples, only Penalty and ApproxGrad converge to the optimal solution and GD and RMD converge to non-

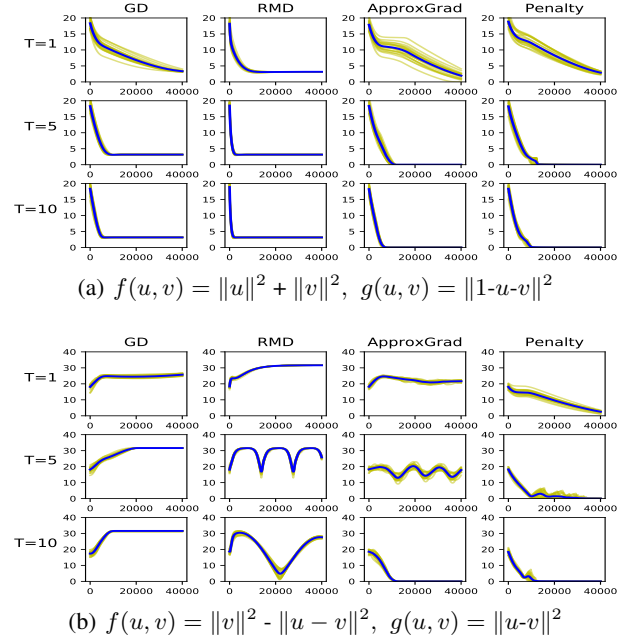


Figure 1. Convergence of GD, RMD, ApproxGrad, and Penalty for two example bilevel problems after 40000 epochs. The mean curve (blue) is superimposed on 20 independent trials (yellow).

solution points (regardless of T). Moreover, from Fig. 1(b), we see that Penalty converges even with $T=1$ while ApproxGrad requires at least $T=10$ to converge, which shows that our method approximates the hypergradient accurately with smaller T . This directly translates to smaller run-time for our method as compared to ApproxGrad since the run-time is directly proportional to T (see Table. 1). In Fig. 2 we show examples similar to Fig. 1 but with ill-conditioned or singular Hessian $\nabla_{vv}^2 g$ for the lower-level problem. The ill-conditioning poses difficulty for the methods since the implicit function theorem requires the invertibility of the Hessian at the solution point. Compared to Fig. 1, Fig. 2 shows that only Penalty converges to the true solution despite the fact that we add regularization $\nabla_{vv}^2 g + \lambda I$ in Ap-

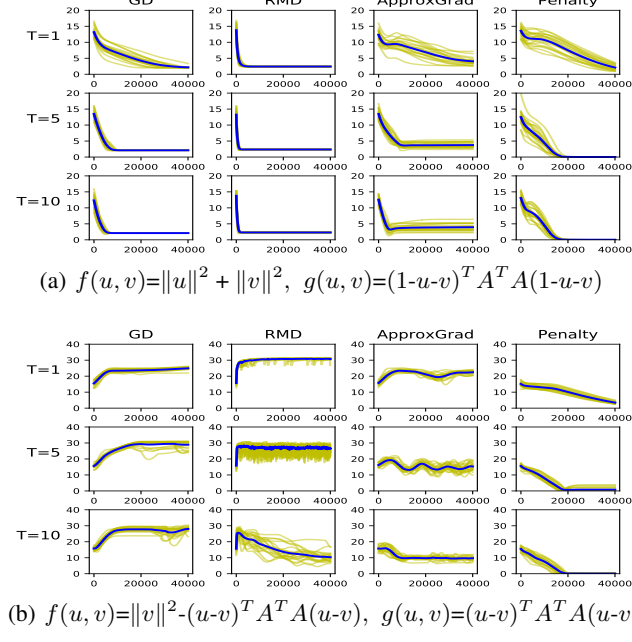


Figure 2. Convergence of GD, RMD, ApproxGrad, and Penalty for two example bilevel problems where $A^T A$ is a rank-deficient random matrix after 40000 epochs. The mean curve (blue) is superimposed on 20 independent trials (yellow).

proxGrad to improve the ill-conditioning when solving the linear systems by minimization. We ascribe the robustness of Penalty to its simplicity and to the fact that it naturally handles non-uniqueness of the lower-level solution (see Appendix C.3). Additionally, we report the wall clock times for different methods on the four examples tested here in Table 2. We can see that as we increase the number of lower-level iterations all methods get slower but Penalty is faster than both RMD and ApproxGrad. Although, Penalty is slower than GD but as shown in Fig. 1 and Fig. 2, GD does not converge to optima for most of the synthetic examples.

3.2. Data denoising by importance learning

Now, we evaluate the performance of Penalty for learning a classifier from a dataset with corrupted labels (training data). We pose the problem as an importance learning problem presented in Eq. (3). We evaluate the performance of the classifier learned by Penalty, with 20 lower-level updates, against the following classifiers: **Oracle**: classifier trained on the portion of training data with clean labels and the validation data, **Val-only**: classifier trained only on the validation data, **Train+Val**: classifier trained on the entire training and validation data, **ApproxGrad**: classifier trained with our implementation of ApproxGrad, with 20 lower-level and 20 linear system updates. We test the performance on MNIST, CIFAR10 and SVHN datasets with validation set

Table 2. Mean wall-clock time (sec) for 10,000 upper-level iterations for synthetic experiments. Boldface is the smallest among RMD, ApproxGrad, and Penalty. (Mean \pm s.d. of 10 runs)

Example 1	GD	RMD	ApproxGrad	Penalty
T=1	7.4 \pm 0.3	15.0\pm0.1	17.4 \pm 0.2	17.2 \pm 0.1
	14.3 \pm 0.1	51.4 \pm 0.3	39.3 \pm 2.3	34.3\pm0.3
	23.2 \pm 0.1	95.4 \pm 0.2	60.9 \pm 0.3	57.0\pm1.0
Example 2	GD	RMD	ApproxGrad	Penalty
T=1	7.7 \pm 0.1	18.5 \pm 0.1	17.2\pm0.3	17.4 \pm 0.2
	17.3 \pm 0.1	62.7 \pm 0.1	37.9 \pm 0.1	35.0\pm0.2
	22.4 \pm 2.6	115.0 \pm 0.4	64.2 \pm 0.3	52.7\pm1.4
Example 3	GD	RMD	ApproxGrad	Penalty
T=1	8.2 \pm 0.2	18.8\pm0.1	19.8 \pm 0.1	19.1 \pm 0.1
	17.4 \pm 0.1	72.4 \pm 0.1	47.1 \pm 0.4	38.6\pm0.4
	28.7 \pm 0.6	125.0 \pm 9.3	80.6 \pm 0.3	62.7\pm0.1
Example 4	GD	RMD	ApproxGrad	Penalty
T=1	7.9 \pm 0.1	19.5\pm0.1	20.4 \pm 0.0	19.6 \pm 0.1
	16.9 \pm 0.2	72.8 \pm 0.5	48.4 \pm 0.6	40.2\pm0.1
	28.3 \pm 0.2	138.0 \pm 0.2	81.2 \pm 1.6	58.0\pm4.3

sizes of 1000, 10000 and 1000 points respectively. We used convolutional neural networks (architectures described in Appendix E.2) at the lower-level for this task. Table 3 summarizes our results for this problem and shows that Penalty outperforms Val-only, Train+Val and ApproxGrad by significant margins and in fact performs very close to the Oracle classifier (which is the ideal classifier), even for high noise levels. This demonstrates that Penalty is extremely effective in solving bilevel problems involving several million variables (see Table 7 in Appendix) and shows its effectiveness at handling non-convex problems. Along with improvement in terms of accuracy over other bilevel methods like ApproxGrad, Penalty also gives better run-time per upper-level iteration, leading to a decrease in the overall wall-clock time of the experiments (Fig. 4(a) in Appendix D).

We compared Penalty against the recent method of Ren et al. which uses a meta-learning based approach and assigns weights to examples based on their gradient directions. We used the same setting as their uniform flip experiment with 36% label noise on CIFAR dataset and Wide ResNet 28-10 (WRN-28-10) model (see Appendix E.2). Using $T=1$ for Penalty and 1000 validation points, we get an accuracy of 87.41 ± 0.26 (mean \pm s.d. of 5 trials) higher than 86.92 ± 0.19 reported by them. Due to the enormous size of WRN-28-10, we do not use larger values of T , but expect it to only improve the results based on the Fig. 4(a) in Appendix D. We also compared Penalty against the RMD-based method of Franceschi et al., using the same setting as their Sec. 5.1, on a subset of MNIST data corrupted with 50% label noise and softmax regression as the model (see Appendix E.2). The accuracy of the classifier trained on a subset of the data with points having importance values greater than 0.9 (as computed by Penalty with $T = 20$) along with the validation set is 90.77% better than 90.09% reported by the RMD-based method.

Table 3. Test accuracy (%) of the classifier learnt from datasets with noisy labels using importance learning. (Mean \pm s.d. of 5 runs)

Dataset (Noise%)	Oracle	Val-Only	Train+Val	Bilevel Approaches	
				ApproxGrad	Penalty
MNIST (25)	99.3 \pm 0.1	90.5 \pm 0.3	83.9 \pm 1.3	98.11 \pm 0.08	98.89\pm0.04
MNIST (50)	99.3 \pm 0.1	90.5 \pm 0.3	60.8 \pm 2.5	97.27 \pm 0.15	97.51\pm0.07
CIFAR10 (25)	82.9 \pm 1.1	70.3 \pm 1.8	79.1 \pm 0.8	71.59 \pm 0.87	79.67\pm1.01
CIFAR10 (50)	80.7 \pm 1.2	70.3 \pm 1.8	72.2 \pm 1.8	68.08 \pm 0.83	79.03\pm1.19
SVHN (25)	91.1 \pm 0.5	70.6 \pm 1.5	71.6 \pm 1.4	80.05 \pm 1.37	88.12\pm0.16
SVHN (50)	89.8 \pm 0.6	70.6 \pm 1.5	47.9 \pm 1.3	74.18 \pm 1.05	85.21\pm0.34

 Table 4. Few-shot classification accuracy (%) on Omniglot and Mini-ImageNet. We report mean \pm s.d. for Omniglot and 95% confidence intervals for Mini-Imagenet over five trials. Results for learning a common representation using Penalty, ApproxGrad and RMD[Franceschi et al., 2018] are averaged over 600 randomly-sampled tasks from the meta-test set. Results for previous methods using similar models are also reported (MAML[Finn et al., 2017], iMAML[Rajeswaran et al., 2019], Prototypical Networks (Proto Net)[Snell et al., 2017], Relation Networks (Rel Net)[Sung et al., 2018], SNAIL[Mishra et al., 2017]).

	MAML	iMAML	Proto Net	Rel Net	SNAIL	Learning a common representation		
						RMD	ApproxGrad	Penalty
Omniglot								
5-way 1-shot	98.7	99.50\pm0.26	98.8	99.6\pm0.2	99.1	98.6	97.75 \pm 0.06	97.83 \pm 0.35
5-way 5-shot	99.9	99.74 \pm 0.11	99.7	99.8\pm0.1	99.8	99.5	99.51\pm0.05	99.45\pm0.05
20-way 1-shot	95.8	96.18 \pm 0.36	96.0	97.6\pm0.2	97.6	95.5	94.69 \pm 0.22	94.06 \pm 0.17
20-way 5-shot	98.9	99.14 \pm 0.10	98.9	99.1 \pm 0.1	99.4	98.4	98.46\pm0.08	98.47\pm0.08
Mini-Imagenet								
5-way 1-shot	48.70 \pm 1.75	49.30 \pm 1.88	49.42 \pm 0.78	50.44 \pm 0.82	55.71\pm0.99	50.54 \pm 0.85	43.74 \pm 1.75	53.17\pm0.96
5-way 5-shot	63.11 \pm 0.92	-	68.20 \pm 0.66	65.32 \pm 0.82	68.88\pm0.92	64.53 \pm 0.68	65.56 \pm 0.67	67.74\pm0.71

3.3. Few-shot learning

Next, we evaluate the performance of Penalty on the task of learning a common representation for the few-shot learning problem. We use the formulation presented in Eq. (4) and use Omniglot [Lake et al., 2015] and Mini-ImageNet [Vinyals et al., 2016] datasets for our experiments. Following the protocol proposed by [Vinyals et al., 2016] for N -way K -shot classification, we generate meta-training and meta-testing datasets. Each meta-set is built using images from disjoint classes. For Omniglot, our meta-training set comprises of images from the first 1200 classes and the remaining 423 classes are used in the meta-testing dataset. We also augment the meta-datasets with three different rotations (90, 180 and 270 degrees) of the images as used by [Santoro et al., 2016]. For the experiments with Mini-Imagenet, we used the split of 64 classes in meta-training, 16 classes in meta-validation and 20 classes in meta-testing as used by [Ravi & Larochelle, 2017].

Each meta-batch of the meta-training and meta-testing dataset comprises of a number of tasks which is called the meta-batch-size. Each task in the meta-batch consists of a training set with K images and a testing set consists of 15 images from N classes. We train Penalty using a meta-batch-size of 30 for 5 way and 15 for 20 way classification for Omniglot and with a meta-batch-size of 2 for Mini-ImageNet experiments. The training sets of the meta-train-batch are used to train the lower-level problem and

the test sets are used as validation sets for the upper-level problem in Eq. (4). The final accuracy is reported using the meta-test-set, for which we fix the common representation learnt during meta-training. We then train the classifiers at the lower-level for 100 steps using the training sets from the meta-test-batch and evaluate the performance of each task on the associated test set from the meta-test-batch. Average performance of Penalty and ApproxGrad over 600 tasks is reported in Table 4. Penalty outperforms other bilevel methods namely the ApproxGrad (trained with 20 lower-level iterations and 20 updates for the linear system) and the RMD-based method [Franceschi et al., 2018] on Mini-Imagenet and is comparable to them on the Omniglot. We also show the trade-off between using higher T and time for ApproxGrad and Penalty (Fig. 4(b) in Appendix D)) showing that Penalty achieves the same accuracy as ApproxGrad in almost half the run-time. In comparison to non-bilevel approaches which used models of the similar size as ours, Penalty is comparable to most approaches and is only slightly worse than [Mishra et al., 2017] which makes use of temporal convolutions and soft attention. We used four-layer convolutional neural networks with 64 filters per layer and a residual network with four residual blocks consisting of 64, 96, 128 and 256 filters followed by two convolutional layers for learning the common task representation (upper-level) for Omniglot and Mini-ImageNet, respectively and use logistic regression to learn task specific classifiers (lower-level).

Table 5. Test accuracy (%) of untargeted poisoning attack (TOP) and success rate (%) of targeted attack (BOTTOM), using MNIST and logistic regression (Mean \pm s.d. of 5 runs). Results for RMD are from [Muñoz-González et al., 2017].

Untargeted Attacks (lower accuracy is better)				
Poisoned points	Label flipping	RMD	ApproxGrad	Penalty
1%	86.71 \pm 0.32	85	82.09 \pm 0.84	83.29 \pm 0.43
2%	86.23 \pm 0.98	83	77.54 \pm 0.57	78.14 \pm 0.53
3%	85.17 \pm 0.96	82	74.41 \pm 1.14	75.14 \pm 1.09
4%	84.93 \pm 0.55	81	71.88 \pm 0.40	72.70 \pm 0.46
5%	84.39 \pm 1.06	80	68.69 \pm 0.86	69.48 \pm 1.93
6%	84.64 \pm 0.69	79	66.91 \pm 0.89	67.59 \pm 1.17
Targeted Attacks (higher accuracy is better)				
Poisoned points	Label flipping	RMD	ApproxGrad	Penalty
1%	7.76 \pm 1.07	10	18.84 \pm 1.90	17.40 \pm 3.00
2%	12.08 \pm 2.13	15	39.64 \pm 3.72	41.64 \pm 4.43
3%	18.36 \pm 1.23	25	52.76 \pm 2.69	51.40 \pm 2.72
4%	24.41 \pm 2.05	35	60.01 \pm 1.61	61.16 \pm 1.34
5%	30.41 \pm 4.24	-	65.61 \pm 4.01	65.52 \pm 2.85
6%	32.88 \pm 3.47	-	71.48 \pm 4.24	70.01 \pm 2.95

3.4. Training-data poisoning

Finally, we evaluate Penalty on the task of generating poisoned training data, such that models trained on this data, perform poorly/differently as compared to the models trained on the clean data. We use the same setting as Sec. 4.2 of [Muñoz-González et al., 2017] and test both untargeted and targeted data poisoning on MNIST using data augmentation technique. We assume regularized logistic regression will be the classifier used for training. The poisoned points obtained after solving Eq. (5) by various methods are added to the clean training set and the performance of a new classifier trained on this data is used to report the results in Table 5. For untargeted attack, our aim is to generally lower the performance of the classifier on the clean test set. For this experiment, we select a random subset of 1000 training, 1000 validation and 8000 testing points from MNIST and initialize the poisoning points with random instances from the training set but assign them incorrect random labels. We use these poisoned points along with clean training data to train logistic regression, in the lower-level problem of Eq. (5). For targeted attacks, we aim to misclassify images of eights as threes. For this, we selected a balanced subset (each of the 10 classes are represented equally in the subset) of 1000 training, 4000 validation and 5000 testing points from the MNIST dataset. Then we select images of class 8 from the validation set and label them as 3 and use only these images for the upper-level problem in Eq. 5 with a difference that now we want to minimize the error in the upper level instead of maximizing (we don't have a negative sign in the upper level of Eq. 5). To evaluate the performance we selected images of 8 from the test set and labeled them as 3

and report the performance on this modified subset of the original test set in targeted attack section of Table 5. For this experiment the poisoned points are initialized with images of classes 3 and 8 from the training set, with flipped labels. This is because images of threes and eights are the only ones involved in the poisoning. We compare the performance of Penalty against the performance reported using RMD in [Muñoz-González et al., 2017] and ApproxGrad. For ApproxGrad, we used 20 lower-level and 20 linear system updates to report the results in the Table 5. We see that Penalty significantly outperforms the RMD based method and performs similar to ApproxGrad. However, in terms of wall clock time Penalty has a advantage over ApproxGrad (see Fig. 4(c) in Appendix D). We also compared the methods against a label flipping baseline where we select poisoned points from the validation sets and change their labels (randomly for untargeted attacks and mislabel threes as 8 and eights as 3 for targeted attacks). All bilevel methods are able to beat this baseline showing that solving the bilevel problem generates better poisoning points. Examples of the poisoned points for untargeted and targeted attacks generated by Penalty are shown in Figs. 5 and 6 in Appendix E.4. Additionally, we tested Penalty on the task of generating clean label poisoning attack [Koh & Liang, 2017; Shafahi et al., 2018] where goal is to learn poisoned points, such that they will be assigned correct labels when visually inspected by an expert, but can cause misclassification of specific target images when the classifier is trained on these poisoned points along with clean data (Appendix E.4.1). We used the dog vs. fish dataset and followed the setting in Sec. 5.2 of [Koh & Liang, 2017], to achieve 100% attack success with just a single poisoned point per target image, compared to 57% attack success in the [Koh & Liang, 2017]. [Shafahi et al., 2018] also report 100% attack success on this task.

4. Conclusion

A wide range of interesting machine learning problems can be expressed as bilevel optimization problems, and new applications are still being discovered. So far, the difficulty of solving bilevel optimization has limited its wide-spread use for solving large-scale problems, specially, involving deep models. In this paper we presented an efficient algorithm based on penalty function to solve bilevel optimization, which is both simple and has theoretical and practical advantages over existing methods. As compared to previous methods we demonstrated competitive performance on problems with convex lower-level costs and significant improvement on problems with non-convex lower-level costs both in terms of accuracy and time, highlighting the practical effectiveness of our penalty-based method. In future works, we plan to tackle other challenges in bilevel optimization such as handling additional constraints in both upper- and lower-levels.

References

Aiyoshi, E. and Shimizu, K. A solution method for the static constrained stackelberg problem via penalty method. *IEEE Transactions on Automatic Control*, 29(12):1111–1114, 1984.

Bard, J. F. Some properties of the bilevel programming problem. *Journal of optimization theory and applications*, 68(2):371–378, 1991.

Bard, J. F. *Practical bilevel optimization: algorithms and applications*, volume 30. Springer Science & Business Media, 2013.

Bertsekas, D. P. On penalty and multiplier methods for constrained minimization. *SIAM Journal on Control and Optimization*, 14(2):216–235, 1976.

Bertsekas, D. P. Nonlinear programming. *Journal of the Operational Research Society*, 48(3):334–334, 1997.

Dempe, S. and Dutta, J. Is bilevel programming a special case of a mathematical program with complementarity constraints? *Mathematical programming*, 131(1-2):37–48, 2012.

Deng, J., Dong, W., Socher, R., Li, L.-J., Li, K., and Fei-Fei, L. Imagenet: A large-scale hierarchical image database. In *2009 IEEE conference on computer vision and pattern recognition*, pp. 248–255. Ieee, 2009.

Domke, J. Generic methods for optimization-based modeling. In *Artificial Intelligence and Statistics*, pp. 318–326, 2012.

Finn, C., Abbeel, P., and Levine, S. Model-agnostic meta-learning for fast adaptation of deep networks. In *International Conference on Machine Learning*, pp. 1126–1135, 2017.

Franceschi, L., Donini, M., Frasconi, P., and Pontil, M. Forward and reverse gradient-based hyperparameter optimization. In *International Conference on Machine Learning*, pp. 1165–1173, 2017.

Franceschi, L., Frasconi, P., Salzo, S., Grazzi, R., and Pontil, M. Bilevel programming for hyperparameter optimization and meta-learning. In *International Conference on Machine Learning*, pp. 1563–1572, 2018.

Hamm, J. and Noh, Y.-K. K-beam minimax: Efficient optimization for deep adversarial learning. *International Conference on Machine Learning (ICML)*, 2018.

Ishizuka, Y. and Aiyoshi, E. Double penalty method for bilevel optimization problems. *Annals of Operations Research*, 34(1):73–88, 1992.

Koh, P. W. and Liang, P. Understanding black-box predictions via influence functions. In *International Conference on Machine Learning*, pp. 1885–1894, 2017.

Lake, B. M., Salakhutdinov, R., and Tenenbaum, J. B. Human-level concept learning through probabilistic program induction. *Science*, 350(6266):1332–1338, 2015.

Liu, T. and Tao, D. Classification with noisy labels by importance reweighting. *IEEE Transactions on pattern analysis and machine intelligence*, 38(3):447–461, 2016.

Luketina, J., Berglund, M., Greff, K., and Raiko, T. Scalable gradient-based tuning of continuous regularization hyperparameters. In *International Conference on Machine Learning*, pp. 2952–2960, 2016.

Luo, C., Zhan, J., Xue, X., Wang, L., Ren, R., and Yang, Q. Cosine normalization: Using cosine similarity instead of dot product in neural networks. In *International Conference on Artificial Neural Networks*, pp. 382–391. Springer, 2018.

MacLaurin, D., Duvenaud, D., and Adams, R. Gradient-based hyperparameter optimization through reversible learning. In *International Conference on Machine Learning*, pp. 2113–2122, 2015.

Mei, S. and Zhu, X. Using machine teaching to identify optimal training-set attacks on machine learners. In *AAAI*, pp. 2871–2877, 2015.

Mishra, N., Rohaninejad, M., Chen, X., and Abbeel, P. A simple neural attentive meta-learner. *arXiv preprint arXiv:1707.03141*, 2017.

Muñoz-González, L., Biggio, B., Demontis, A., Paudice, A., Wongrassamee, V., Lupu, E. C., and Roli, F. Towards poisoning of deep learning algorithms with back-gradient optimization. In *Proceedings of the 10th ACM Workshop on Artificial Intelligence and Security*, pp. 27–38. ACM, 2017.

Nocedal, J. and Wright, S. *Numerical optimization*. Springer Science & Business Media, 2006.

Pearlmutter, B. A. Fast exact multiplication by the hessian. *Neural computation*, 6(1):147–160, 1994.

Pedregosa, F. Hyperparameter optimization with approximate gradient. In *International conference on machine learning*, pp. 737–746, 2016.

Rajeswaran, A., Finn, C., Kakade, S. M., and Levine, S. Meta-learning with implicit gradients. In *Advances in Neural Information Processing Systems*, pp. 113–124, 2019.

Ravi, S. and Larochelle, H. Optimization as a model for few-shot learning. *International Conference on Learning Representations (ICLR)*, 2017.

Ren, M., Zeng, W., Yang, B., and Urtasun, R. Learning to reweight examples for robust deep learning. In *ICML*, 2018.

Santoro, A., Bartunov, S., Botvinick, M., Wierstra, D., and Lillicrap, T. One-shot learning with memory-augmented neural networks. *arXiv preprint arXiv:1605.06065*, 2016.

Shaban, A., Cheng, C.-A., Hatch, N., and Boots, B. Truncated back-propagation for bilevel optimization. *arXiv preprint arXiv:1810.10667*, 2018.

Shafahi, A., Huang, W. R., Najibi, M., Suciu, O., Studer, C., Dumitras, T., and Goldstein, T. Poison frogs! targeted clean-label poisoning attacks on neural networks. In *Advances in Neural Information Processing Systems*, pp. 6103–6113, 2018.

Snell, J., Swersky, K., and Zemel, R. Prototypical networks for few-shot learning. In *Advances in Neural Information Processing Systems*, pp. 4080–4090, 2017.

Sung, F., Yang, Y., Zhang, L., Xiang, T., Torr, P. H., and Hospedales, T. M. Learning to compare: Relation network for few-shot learning. In *Proceedings of the IEEE Conference on Computer Vision and Pattern Recognition*, pp. 1199–1208, 2018.

Vinyals, O., Blundell, C., Lillicrap, T., Wierstra, D., et al. Matching networks for one shot learning. In *Advances in Neural Information Processing Systems*, pp. 3630–3638, 2016.

von Stackelberg, H. *Market structure and equilibrium*. Springer Science & Business Media, 2010.

Yu, X., Liu, T., Gong, M., Zhang, K., and Tao, D. Transfer learning with label noise. *arXiv preprint arXiv:1707.09724*, 2017.

Appendix

We provide missing proofs in Appendix A, a review of other methods of hypergradient computation in Appendix B, discuss modifications to improve the Alg. 1 in Appendix C, and the experiment details and additional results in Appendix E.

A. Proofs

Theorem 2. Suppose $\{\epsilon_k\}$ is a positive ($\epsilon > 0$) and convergent ($\epsilon_k \rightarrow 0$) sequence, and $\{\gamma_k\}$ is a positive ($\gamma_k > 0$), non-decreasing ($\gamma_1 \leq \gamma_2 \leq \dots$), and a divergent ($\gamma_k \rightarrow \infty$) sequence. Let $\{(u_k, v_k)\}$ be the sequence of approximate solutions to Eq. (9) with tolerance $(\nabla_w \tilde{f}(u_k, v_k))^2 + (\nabla_v \tilde{f}(u_k, v_k))^2 \leq \epsilon_k^2$ for all $k = 0, 1, \dots$. Then any limit point of $\{(u_k, v_k)\}$ satisfies the KKT conditions of the problem Eq. (8).

Proof. The proof follows the standard proof for penalty function methods, e.g., [Nocedal & Wright, 2006]. Let $w := (u, v)$ refer to the pair, and let $\bar{w} := (\bar{u}, \bar{v})$ be any limit point of the sequence $\{w_k := (u_k, v_k)\}$, then there is a subsequence \mathcal{K} such that $\lim_{k \in \mathcal{K}} w_k = \bar{w}$. From the tolerance condition

$$\begin{aligned} \|\nabla_w \tilde{f}(w_k; \gamma_k)\| = \\ \|\nabla_w f(w_k) + \gamma_k \nabla_{wv}^2 g(w_k) \nabla_v g(w_k)\| \leq \epsilon_k \end{aligned}$$

we have

$$\|\nabla_{wv}^2 g(w_k) \nabla_v g(w_k)\| \leq \frac{1}{\gamma_k} [\|\nabla_w f(w_k)\| + \epsilon_k]$$

Take the limit with respect to the subsequence \mathcal{K} on both sides to get

$$\nabla_{wv}^2 g(\bar{w}) \nabla_v g(\bar{w}) = 0$$

Since $\nabla_{wv}^2 g = \begin{pmatrix} \nabla_{uv}^2 g \\ \nabla_{vv}^2 g \end{pmatrix}$ is a tall matrix and $\nabla_{vv}^2 g$ is invertible by assumption, $\nabla_{wv}^2 g$ is full-rank and therefore $\nabla_v g(\bar{w}) = 0$, which is the primary feasibility condition in Eq. (8). Furthermore, let $\mu_k := -\gamma_k \nabla_v g(w_k)$, then by definition,

$$\nabla_w \tilde{f}(w_k; \gamma_k) = \nabla_w f(w_k) - \nabla_{wv}^2 g(w_k) \mu_k$$

We can write

$$\begin{aligned} [\nabla_{wv}^2 g(w_k)^T \nabla_{wv}^2 g(w_k)] \mu_k = \\ \nabla_{wv}^2 g(w_k)^T [\nabla_w f(w_k) - \nabla_w \tilde{f}(w_k; \gamma_k)] \end{aligned}$$

The corresponding limit $\bar{\mu}$ can be found by taking the limit of the subsequence \mathcal{K}

$$\begin{aligned} \bar{\mu} := \lim_{k \in \mathcal{K}} \mu_k = \\ [\nabla_{wv}^2 g(\bar{w})^T \nabla_{wv}^2 g(\bar{w})]^{-1} \nabla_{wv}^2 g(\bar{w})^T \nabla_w f(\bar{w}) \end{aligned}$$

Since $\lim_{k \in \mathcal{K}} \nabla_w \tilde{f}(w_k; \gamma_k) = 0$ from the condition $\epsilon_k \rightarrow 0$, we get

$$\nabla_w f(\bar{w}) - \nabla_{wv}^2 g(\bar{w}) \bar{\mu} = 0$$

at the limit \bar{w} , which is the stationarity condition of Eq. (8). Together with the feasibility condition $\nabla_v g(\bar{w}) = 0$, the two KKT conditions of Eq. (8) are satisfied at the limit point. \square

Lemma 3. Given u , let \hat{v} be $\hat{v} := \arg \min_v \tilde{f}(u, v; \gamma)$ of Eq. (9). Then, $\nabla_u \tilde{f}(u, \hat{v}; \gamma) = \frac{df}{du}(u, \hat{v})$.

Proof. At the minimum \hat{v} the gradient $\nabla_v \tilde{f}$ vanishes, that is $\nabla_v f + \gamma \nabla_{vv}^2 g \nabla_v g = 0$.

Equivalently, $\nabla_v g = -\gamma^{-1} (\nabla_{vv}^2 g)^{-1} \nabla_v f$. Then,

$$\begin{aligned} \nabla_u \tilde{f}(\hat{v}) &= \nabla_u f(\hat{v}) + \gamma \nabla_{uv}^2 g(\hat{v}) \nabla_v g(\hat{v}) = \\ \nabla_u f(\hat{v}) - \nabla_{uv}^2 g(\hat{v}) \nabla_{vv}^2 g^{-1}(\hat{v}) \nabla_v f(\hat{v}), \end{aligned}$$

where γ disappears, which is the hypergradient $\frac{df}{du}(u, \hat{v})$. \square

That is, if we find the minimum \hat{v} of the penalty function for given u and γ , we get the hypergradient Eq. (7) at (u, \hat{v}) . Furthermore, under the conditions of Theorem 1, $\hat{v}(u) \rightarrow v^*(u)$ as $\gamma \rightarrow \infty$ (see Lemma 8.3.1 of [Bard, 2013]), and we get the exact hypergradient asymptotically.

B. Review of other bilevel optimization methods

Several methods have been proposed to solve bilevel optimization problems appearing in machine learning, including forward/reverse-mode differentiation [Maclaurin et al., 2015; Franceschi et al., 2017] and approximate gradient [Domke, 2012; Pedregosa, 2016] described briefly here.

Forward-mode (FMD) and Reverse-mode differentiation (RMD). Domke [Domke, 2012], Maclaurin et al. [Maclaurin et al., 2015], Franceschi et al. [Franceschi et al., 2017], and Shaban et al. [Shaban et al., 2018] studied forward and reverse-mode differentiation to solve the minimization problem $\min_u f(u, v)$ where the lower-level variable v follows a dynamical system $v_{t+1} = \Phi_{t+1}(v_t; u)$, $t = 0, 1, 2, \dots, T-1$. This setting is more general than that of a bilevel problem. However, a stable dynamical system is one that converges to a steady state and thus, the process $\Phi_{t+1}(\cdot)$ can be considered as minimizing an energy or a potential function.

Define $A_{t+1} := \nabla_v \Phi_{t+1}(v_t)$ and $B_{t+1} := \nabla_u \Phi_{t+1}(v_t)$, then the hypergradient Eq. (7) can be computed by

$$\frac{df}{du} = \nabla_u f(u, v_T) + \sum_{t=0}^T B_t A_{t+1} \times \dots \times A_T \nabla_v f(u, v_T)$$

When the lower-level process is one step of gradient descent on a cost function g , that is,

$$\Phi_{t+1}(v_t; u) = v_t - \rho \nabla_v g(u, v_t)$$

we get

$$A_{t+1} = I - \rho \nabla_{vv}^2 g(u, v_t), \quad B_{t+1} = -\rho \nabla_{uv}^2 g(u, v_t).$$

A_t is of dimension $V \times V$ and B_t is of dimension $V \times U$. The sequences $\{A_t\}$ and $\{B_t\}$ can be computed in forward or reverse mode. For reverse-mode differentiation, first compute

$$v_{t+1} = \Phi_{t+1}(v_t), \quad t = 0, 1, \dots, T-1,$$

then compute

$$\begin{aligned} q_T &\leftarrow \nabla_v f(u, v_T), \quad p_T \leftarrow \nabla_u f(u, v_T) \\ p_{t-1} &\leftarrow p_t + B_t q_t, \quad q_{t-1} \leftarrow A_t q_t, \quad t = T, T-1, \dots, 1. \end{aligned}$$

Time and space Complexity for computing p_t is $O(V)$ since the Jacobian vector product can be computed in $O(V)$ time and space. The final hypergradient for RMD is $\frac{df}{du} = p_0$. Hence the final time complexity for RMD is $O(VT)$ and space complexity is $O(U + VT)$.

For forward-mode differentiation, simultaneously compute v_t, A_t, B_t and

$$P_0 \leftarrow 0, \quad P_{t+1} \leftarrow P_t A_{t+1} + B_{t+1}, \quad t = 0, 1, \dots, T-1.$$

Time complexity for computing P_t is $O(UV)$ since $P_t A_{t+1}$ can be computed using U Hessian vector products each needing $O(V)$ and B_{t+1} also needs $O(UV)$ using unit vectors e_i for $i = 1 \dots U$. The space complexity for each P_t is $O(UV)$. The final hypergradient for FMD is

$$\frac{df}{du} = \nabla_u f(u, v_T) + P_T \nabla_v f(v_T).$$

Hence the final time complexity for FMD is $O(UVT)$ and space complexity is $O(U + UV) = O(UV)$.

Approximate hypergradient (ApproxGrad). Since computing the inverse of the Hessian $(\nabla_{vv}^2 g)^{-1}$ directly is difficult even for moderately-sized neural networks, Domke [Domke, 2012] proposed to find an approximate solution to $q = (\nabla_{vv}^2 g)^{-1} \nabla_v f$ by solving the linear system of equations $\nabla_{vv}^2 g \cdot q \approx \nabla_v f$. This can be done by solving

$$\min_q \|\nabla_{vv}^2 g \cdot q - \nabla_v f\|$$

using gradient descent, conjugate gradient descent or any other iterative solver. Note that the minimization requires evaluation of the Hessian-vector product, which can be done in linear time [Pearlmutter, 1994]. Hence the time complexity of the method is $O(VT)$ and space complexity is $O(U + V)$ since we only need to store single copy of u and v same as Penalty. The asymptotic convergence with approximate solutions was shown by Pedregosa [Pedregosa, 2016].

C. Improvements to Algorithm 1

Here we discuss the details of the modifications to Alg. 1 presented in the main text which can be added to improve the performance of the algorithm in practice.

C.1. Improving local convexity by regularization

One of the common assumptions of this and previous works is that $\nabla_{vv}^2 g$ is invertible and locally positive definite. Neither invertibility nor positive definiteness hold in general for bilevel problems, involving deep neural networks, and this causes difficulties in the optimization. Note that if g is non-convex in v , minimizing the penalty term $\|\nabla_v g\|$ does not necessarily lower the cost g but instead just moves the variable towards a stationary point – which is a known problem even for the Newton’s method. Thus we propose the following modification to the v -update:

$$\min_v \left[f + \frac{\gamma_k}{2} \|\nabla_v g\|^2 + \lambda_k g \right]$$

keeping the u -update intact. To see how this affects the optimization, note that v -update becomes

$$v \leftarrow v - \rho [f_v + \gamma_k \nabla_{vv}^2 g \nabla_v g + \lambda_k \nabla_v g]$$

After v converges to a stationary point, we get $\nabla_v g = -(\gamma_k \nabla_{vv}^2 g + \lambda_k I)^{-1} \nabla_v f$, and after plugging this into u -update, we get

$$u \leftarrow u - \sigma \left[\nabla_u f - \nabla_{uv}^2 g \left(\nabla_{vv}^2 g + \frac{\lambda_k}{\gamma_k} I \right)^{-1} \nabla_v f \right]$$

that is, the Hessian inverse $\nabla_{vv}^2 g^{-1}$ is replaced by a regularized version $(\nabla_{vv}^2 g + \frac{\lambda_k}{\gamma_k} I)^{-1}$ to improve the positive definiteness of the Hessian. With a decreasing or constant sequence $\{\lambda_k\}$ such that $\lambda_k/\gamma_k \rightarrow 0$ the regularization does not change to solution.

C.2. Convergence with finite γ_k

The penalty function method is intuitive and easy to implement, but the sequence $\{(\hat{u}_k, \hat{v}_k)\}$ is guaranteed to converge to an optimal solution only in the limit with $\gamma \rightarrow \infty$, which may not be achieved in practice in a limited time. It is known that the penalty method can be improved by introducing an additional term into the function, which is called the augmented Lagrangian (penalty) method [Bertsekas, 1976]:

$$\min_{u,v} \left[f + \frac{\gamma_k}{2} \|\nabla_v g\|^2 + \nabla_v g^T \nu \right].$$

This new term $\nabla_v g^T \nu$ allows convergence to the optimal solution (u^*, v^*) even when γ_k is finite. Furthermore, using the update rule $\nu \leftarrow \nu + \gamma \nabla_v g$, called the method of multipliers, it is known that ν converges to the true Lagrange multiplier of this problem corresponding to the equality constraints $\nabla_v g = 0$.

C.3. Non-unique lower-level solution

Most existing methods have assumed that the lower-level solution $\arg \min_v g(u, v)$ is unique for all u . Regularization from the previous section, can improve the ill-conditioning of the Hessian $\nabla_{vv}^2 g$ but it does not address the case of multiple disconnected global minima of g . With multiple lower-level solutions $Z(u) = \{v \mid v = \arg \min g(u, v)\}$, there is an ambiguity in defining the upper-level problem. If we assume that $v \in Z(u)$ is chosen adversarially (or pessimistically), then the upper-level problem should be defined as

$$\min_u \max_{v \in Z(u)} f(u, v).$$

If $v \in Z(u)$ is chosen co-operatively (or optimistically), then the upper-level problem should be defined as

$$\min_u \min_{v \in Z(u)} f(u, v),$$

and the results can be quite different between these two cases. Note that the proposed penalty function method is naturally solving the optimistic case, as Alg. 1 is solving the problem of $\min_{u, v} \tilde{f}(u, v)$ by alternating gradient descent. However, with a gradient-based method, we cannot hope to find all disconnected multiple solutions. In a related problem of min-max optimization, which is a special case of bilevel optimization, an algorithm for handling non-unique solutions was proposed recently [Hamm & Noh, 2018]. This idea of keeping multiple candidate solution may be applicable to bilevel problems too and further analysis of the non-unique lower-level problem is left as future work.

C.4. Modified algorithm

Here we present the modified algorithm which incorporates regularization (Sec. C.1) and augmented Lagrangian (Sec. C.2) as discussed previously. The augmented Lagrangian term $\nabla_v g^T \nu$ applies to both u - and v -update, but the regularization term λg applies to only the v -update as its purpose is to improve the ill-conditioning of $\nabla_{vv}^2 g$ during v -update. The modified penalized functions \tilde{f}_1 for u -update and \tilde{f}_2 for v -update are

$$\begin{aligned} \tilde{f}_1(u, v; \gamma, \nu) &:= f + \frac{\gamma}{2} \|\nabla_v g\|^2 + \nabla_v g^T \nu \\ \tilde{f}_2(u, v; \gamma, \lambda, \nu) &:= f + \frac{\gamma}{2} \|\nabla_v g\|^2 + \nabla_v g^T \nu + \lambda g \end{aligned}$$

The new algorithm (Alg. 2) is similar to Alg. 1 with additional steps for updating λ_k and ν_k .

C.5. Impact of various hyperparameters and terms

Here we evaluate the impact of different initial values for the hyperparameters and impact of different terms added

Algorithm 2 Modified Alg. 1 with regularization and augmented Lagrangian

Input: $K, T, \{\sigma_k\}, \{\rho_{k,t}\}, \gamma_0, \epsilon_0, \lambda_0, \nu_0, c_\gamma (=1.1), c_\epsilon (=0.9), c_\lambda (=0.9)$

Output: (u_K, v_T)

Initialize u_0, v_0 randomly

Begin

```

for  $k = 0, \dots, K-1$  do
    while  $\|\nabla_u \tilde{f}_1\|^2 + \|\nabla_v \tilde{f}_2\|^2 > \epsilon_k^2$  do
        for  $t = 0, \dots, T-1$  do
             $v_{t+1} \leftarrow v_t - \rho_{k,t} \nabla_v \tilde{f}_2(u_k, v_t)$ 
        end for
         $u_{k+1} \leftarrow u_k - \sigma_k \nabla_u \tilde{f}_1(u_k, v_T)$ 
    end while
     $\gamma_{k+1} \leftarrow c_\gamma \gamma_k$ 
     $\epsilon_{k+1} \leftarrow c_\epsilon \epsilon_k$ 
     $\lambda_{k+1} \leftarrow c_\lambda \lambda_k$ 
     $\nu_{k+1} \leftarrow \nu_k + \gamma_k \nabla_v g$ 
end for

```

in the modified algorithm (Algorithm 2). In particular, we examine the effect of using different initial values of λ_0 for synthetic experiments and λ_0, γ_0 for untargeted data poisoning with 60 points and also test the effect of having the $\lambda_k g$ and $\nabla_v g^T \nu$ (Fig. 3 and Table 6). Based on the results we find that initial value of the regularization parameter λ_0 does not influence the results too much and absence of $\lambda_k g$ ($\lambda_k = 0$) also does not change the results too much. We also don't see significant gains from using the augmented Lagrangian term and method of multipliers on these simple problems. However, the initial value of the parameter γ_0 does influence the results since starting from very large γ_0 makes the algorithm focus only on satisfying the necessary condition at the lower level ignoring the f where as with small γ_0 it can take a large number of iterations for the penalty term to have influence. Apart from these, we also tested the effects of the rate of tolerance decrease (c_ϵ) and penalty increase (c_γ), and initial value for ϵ_0 . Within certain ranges, the results do not change much.

D. Impact of T on accuracy and run-time

Here, we compare the accuracy and time for Penalty and ApproxGrad (Fig. 4) as we vary the number of lower-level iterations T for different experiments. Intuitively, a larger T corresponds to a more accurate approximation of the hypergradient and therefore improves the results for both the methods. But this improvement comes with a significant increase in the time. Moreover, Fig. 4 shows that relative improvement after $T = 20$ is small in comparison to the increased run-time for Penalty and specially for ApproxGrad. Based on these results we used $T = 20$ for all our experiments on real data for both the methods. The figure

Table 6. Effect of using different initial values for various hyperparameters with Penalty on untargeted data poisoning attacks (**lower** accuracy is better) with 60 poisoning points (Mean \pm s.d. of 5 runs with $T = 20$ (lower-level iterations)). We used the parameters corresponding to the bold values for the results reported in Table 5.

Hyper-parameters	Different initial values of various hyperparameters			
	$\lambda_0 = 0$	$\lambda_0 = 1$	$\lambda_0 = 10$	$\lambda_0 = 100$
λ_0	67.87 ± 1.35	68.21 ± 1.78	68.18 ± 1.04	67.59 ± 1.17
ν	with ν		without ν	
	67.59 ± 1.17		68.82 ± 0.75	
γ_0	$\gamma_0 = 1$	$\gamma_0 = 10$	$\gamma_0 = 100$	
	73.38 ± 4.98	67.59 ± 1.17	71.96 ± 3.56	

Table 7. Upper- and lower-level variable sizes for different experiments

Experiment	Dataset	Upper-level variable	Lower-level variable
Data denoising	MNIST	59K	1.4M
	CIFAR10 (Alexnet)	40K	1.2M
	CIFAR10 (WRN-28-10)	44K	36M
	SVHN	72K	1.3M
Few-shot learning	Omniglot	111K	39K
	Mini-Imagenet	3.8M	5K
Data poisoning	MNIST (Augment 60 poison points)	47K	8K
	ImageNet (Clean label attack)	268K	4K

also shows that even though Penalty and ApproxGrad have the same linear time complexity (Table 1), Penalty is about twice as fast ApproxGrad in wall-clock time.

E. Details of experiments

All codes are written in Python using Tensorflow/Keras, and were run on Intel CORE i9-7920X CPU with 128 GB of RAM and dual NVIDIA TITAN RTX. Implementation and hyperparameters of the algorithms are experiment-dependent and described separately below.

E.1. Synthetic examples

In this experiment, four simple bilevel problems with known optimal solutions are used to check the convergence of different algorithms. The two problems in Fig. 1 are

$$\min_{u,v} \|u\|^2 + \|v\|^2, \text{ s.t. } v = \arg \min_v \|1 - u - v\|^2,$$

and

$$\min_{u,v} \|v\|^2 - \|u - v\|^2, \text{ s.t. } v = \arg \min_v \|u - v\|^2,$$

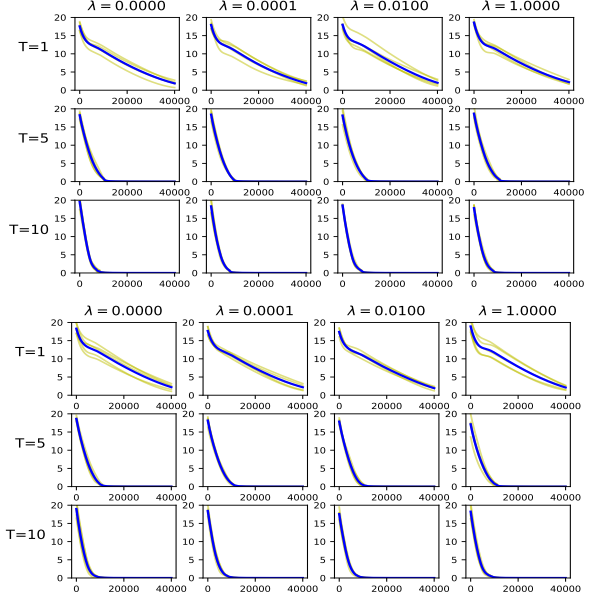


Figure 3. Penalty method for $T=1,5,10$ and $\lambda_0 = 0, 10^{-4}, 10^{-2}, 1$ for Example 1 of Sec.3.1. Top: with ν . Bottom: without ν . Averaged over 5 trials.

where $u = [u_1, \dots, u_{10}]^T$, $|u_i| \leq 5$ and $v = [v_1, \dots, v_{10}]^T$, $|v_i| \leq 5$. The optimal solutions are $u_i = v_i = 0.5$, $i = 1, \dots, 10$ for the former and $u_i = v_i = 0$, $i = 1, \dots, 10$ for the latter. Since there are unique solutions, convergence is measured by the Euclidean distance $\sqrt{\|u - u^*\|^2 + \|v - v^*\|^2}$ of the current iterate (u, v) and the optimal solution (u^*, v^*) .

The two problems in Fig. 2 are

$$\begin{aligned} & \min_{u,v} \|u\|^2 + \|v\|^2, \text{ s.t.} \\ & v = \arg \min_v (1 - u - v)^T A^T A (1 - u - v) \end{aligned}$$

and

$$\begin{aligned} & \min_{u,v} \|v\|^2 - (u - v)^T A^T A (u - v), \text{ s.t.} \\ & v = \arg \min_v (u - v)^T A^T A (u - v), \end{aligned}$$

where A is a 5×10 real matrix such that $A^T A$ is rank-deficient, and the domains are the same as before. These problems are ill-conditioned versions of the previous two problems and are more challenging. The optimal solutions to these two example problems are not unique. For the former, the solutions are $u = 0.5 + p$ and $v = 0.5 + p$ for any vector $p \in \text{Null}(A)$. For the latter, $u = p$ and $v = 0$ for any vector $p \in \text{Null}(A)$. Since they are non-unique, convergence is measured by the residual distance $\sqrt{\|P(u - 0.5)\|^2 + \|P(v - 0.5)\|^2}$ for the former and $\sqrt{\|Pu\|^2 + \|v\|^2}$ for the latter, where

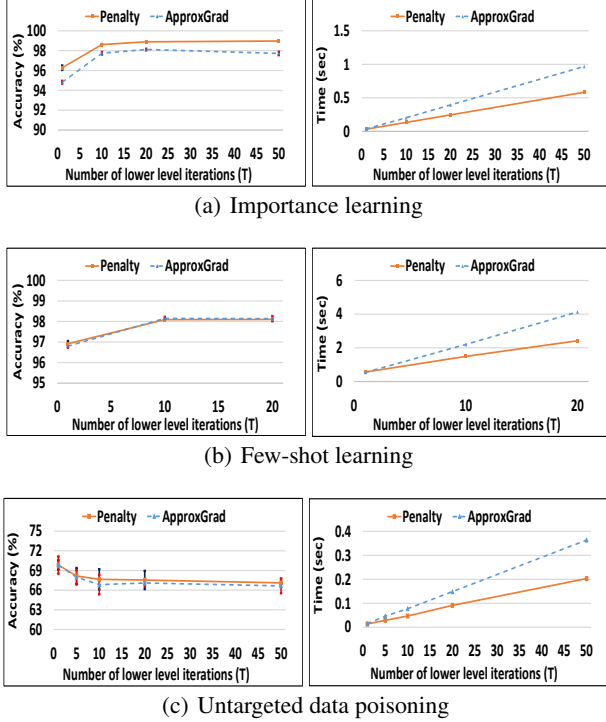


Figure 4. Comparison of accuracy and wall clock time (per upper-level iteration) with number of lower-level iterations T of Penalty and ApproxGrad (for ApproxGrad, we perform T updates for the linear system too.) on data denoising problem (Sec. 3.2 with 25% noise on MNIST), few-shot learning problem (Sec. 3.3 with 20 way 5 shot classification on Omniglot) and untargeted data poisoning (Sec. 3.4 with 60 poisoned points on MNIST).

$P = A^T (A A^T)^{-1} A$ is the orthogonal projection to the row-space of A .

Algorithms used in this experiment are GD, RMD, ApproxGrad, and Penalty. Adam optimizer is used for minimization everywhere except RMD which uses gradient descent for a simpler implementation. The learning rates common to all algorithms are $\sigma_0 = 10^{-3}$ for u -update and $\rho_0 = 10^{-4}$ for v - and p -updates. For Penalty, the values $\gamma_0 = 1$, $\lambda_0 = 10$, and $\epsilon_0 = 1$ are used. For each problem and algorithm, 20 independent trials are performed with random initial locations (u_0, v_0) sampled uniformly in the domain, and random entries of A sampled from independent Gaussian distributions. We test with $T = 1, 5, 10$. Each run was stopped after $K = 40000$ iterations of u -updates.

E.2. Data denoising by importance learning

Following the formulation for data denoising presented in Eq. (3), we associate an importance value (denoted by u_i) with each point in the training data. Our goal is to find the correct values for these u_i 's such that the noisy points are given a lower importance values and clean points are

given a higher importance values. In our experiments, we allow the importance values to be between 0 and 1. We use the change of variable technique to achieve this. We set $u'_i = 0.5(\tanh(u_i) + 1)$ and since $-1 \leq \tanh(u_i) \leq 1$, u'_i is automatically scaled between 0 and 1. We use a warm start for the bilevel methods (Penalty and ApproxGrad) by pre-training the network using the validation set and initializing the importance values with the predicted output probability from the pre-trained network. We see an advantage in convergence speed of the bilevel methods with this pre-training. Below we describe the network architectures used for our experiments.

For the experiments on the MNIST dataset, our network consists of a convolution layer with kernel size of 5×5 , 64 filters and ReLU activation, followed by a max pooling layer of size 2×2 and a dropout layer with drop rate of 0.25. This is followed by another convolution layer with 5×5 kernel, 128 filters and ReLU activation followed by similar max pooling and dropout layers. Then we have 2 fully connected layers with ReLU activation of size 512 and 256 respectively, each followed by a dropout layer with a drop rate of 0.5. Lastly, we have a softmax layer with 10 classes. We used the Adam optimizer with a learning rate of 0.00001, batch size of 200 and 100 epochs to report the accuracy of Oracle, Val-Only and Train+Val classifiers. For bilevel training using Penalty we used $K = 100$, $T = 20$, $\sigma_0=3$, $\rho_0=0.00001$, $\gamma_0=0.01$, $\epsilon_0=0.01$, $\lambda_0=0.01$, $\nu_0=0.000001$ as per Alg. 2.

For the experiments on the CIFAR10 dataset, our network consists of 3 convolution blocks with filter sizes of 48, 96, and 192. Each convolution block consists of two convolution layers, each with kernel size of 3×3 and ReLU activation. This is followed by a max pooling layer of size 2×2 and a drop out layer with drop rate of 0.25. After these 3 blocks we have 2 dense layers with ReLU activation of size 512 and 256 respectively, each followed by a dropout layer with rate 0.5. Finally we have a softmax layer with 10 classes. This is optimized with the Adam optimizer using a learning rate of 0.001 for 200 epochs with batch size of 200 to report the accuracy of Oracle, Val-Only and Train+Val classifiers. For this experiment we used data augmentation during our training. For the bilevel training using Penalty we used $K = 200$, $T = 20$, $\sigma_0=3$, $\rho_0=0.00001$, $\gamma_0=0.01$, $\epsilon_0=0.01$, $\lambda_0=0.01$, $\nu_0=0.00001$ with mini-batches of size 200. We also use data augmentation for bilevel training.

For the experiments on the SVHN dataset, our network consists of 3 blocks each with 2 convolution layers with kernel size of 3×3 and ReLU activation followed by a max pooling and drop out layer (drop rate = 0.3). The two convolution layers of the first block has 32 filters, second block has 64 filters and the last block has 128 filters. This is followed by a dense layer of size 512 with ReLU activation and dropout layer with drop rate = 0.3. Finally we have a softmax layer

with 10 classes. This is optimized with the Adam optimizer and learning rate of 0.001 for 100 epochs to report results of of Oracle, Val-Only and Train+Val classifiers. The bilevel training uses $K = 100$ and $T = 20$, $\sigma_0=3$, $\rho_0=0.00001$, $\gamma_0=0.01$, $\epsilon_0=0.01$, $\lambda_0=0.01$, $\nu_0=0.0$ with batch-size of 200. The test accuracy of these models when trained on the entire training data without any label corruption are 99.5% for MNIST, 86.2% for CIFAR10 and 91.23% for SVHN. For all the experiments with ApproxGrad, we used 20 updates for the lower-level and 20 updates for the linear system and did same number of epochs as for Penalty (i.e. 100 for MNIST and SVHN and 200 for CIFAR), with a mini-batch-size 200.

E.2.1. COMPARISON WITH FRANCESCHI ET AL.

For comparison of Penalty against the RMD-based method presented in [Franceschi et al., 2017], we used their setting from Sec. 5.1, which is a smaller version of this data denoising task. For this, we choose a sample of 5000 training, 5000 validation and 10000 test points from MNIST and randomly corrupted labels of 50% of the training points and used softmax regression in the lower-level of the bilevel formulation (Eq. (3)). The accuracy of the classifier trained on a subset of the dataset comprising only of points with importance values greater than 0.9 (as computed by Penalty) along with the validation set is 90.77%. This is better than the accuracy obtained by Val-only (90.54%), Train+Val (86.25%) and the RMD-based method (90.09%) used by [Franceschi et al., 2017] and is close to the accuracy achieved by Oracle classifier (91.06%). The bilevel training uses $K = 100$ and $T = 20$, $\sigma_0=3$, $\rho_0=0.00001$, $\gamma_0=0.01$, $\epsilon_0=0.01$, $\lambda_0=0.01$, $\nu_0=0.0$ with batch-size of 200

E.2.2. COMPARISON WITH REN ET AL.

To demonstrate the effectiveness of penalty in solving the importance learning problem with bigger models, we compared its performance against the recent method proposed by Ren et al., which uses a meta-learning approach to find the weights for each example in the noisy training set based on their gradient directions. We use the same setting as their uniform flip experiment with 36% label noise on CIFAR dataset. We also use our own implementation of the Wide Resnet 28-10 (WRN-28-10) which achieves roughly 93% accuracy without any label noise. For comparison, we used the validation set of 1000 points and training set of 44000 points with labels of 36% points corrupted, same as used by Ren et al.. We use Penalty with $T = 1$ since using larger T was not possible due to extremely high computational needs. However, using larger value T is expected to imporve the results further based on Fig. 4(a). Different from other experiments in this section we did not use the arc tangent conversion to restrict importance values between 0 and 1 but instead just normalize the importance values in a batch, similar to the method used by Ren et al., for proper com-

parison. We used $K = 200$ and $T = 1$, $\sigma_0=3$, $\rho_0=0.0001$, $\gamma_0=1$, $\epsilon_0=1$, $\lambda_0=10$, $\nu_0=0.0$ with batch-size of 75 and used data augmentation during training. We achieve an accuracy of 87.41 ± 0.26 .

E.3. Few-shot learning

For these experiments, we used the Omniglot [Lake et al., 2015] dataset consisting of 20 instances (size 28×28) of 1623 characters from 50 different alphabets and the Mini-ImageNet [Vinyals et al., 2016] dataset consisting of 60000 images (size 84×84) from 100 different classes of the ImageNet [Deng et al., 2009] dataset. For the experiments on the Omniglot dataset we used a network with 4 convolution layers to learn the common representation for the tasks. The first three layers of the network have 64 filters, batch normalization, ReLU activation and a 2×2 max-pooling. The final layer is same as the previous ones with the exception that it does not have any activation function. The final representation size is 64. For the Mini-ImageNet experiments we used a residual network with 4 residual blocks consisting of 64, 96, 128 and 256 filters followed by a 1×1 convolution block with 2048 filters, average pooling and finally a 1×1 convolution block with 384 filters. Each residual block consists of 3 blocks of 1×1 convolution, batch normalization, leaky ReLU with leak = 0.1, before the residual connection and is followed by dropout with rate = 0.9. The last convolution block does not have any activation function. The final representation size is 384. Similar architectures have been used by [Franceschi et al., 2018] in their work with a difference that we don't use any activation function in the last layers of the representation in our experiments. For both the datasets, the lower-level problem is a softmax regression with a difference that we normalize the dot product of the input representation and the weights with the l_2 -norm of the weights and the l_2 -norm of the input representation, similar to the cosine normalization proposed by [Luo et al., 2018]. For N way classification, the dimension of the weights in the lower-level are $64 \times N$ for Omniglot and $384 \times N$ for Mini-ImageNet. For our Omniglot experiments we use a meta-batch-size 30 for 5-way and 20-way classification and a meta-batch-size of 2 for 5-way classification with Mini-ImageNet. We use $T = 20$ iterations for the lower-level in all experiments and ran them for $K=10000$. The hyper-parameters used for Penalty are $\sigma_0=0.001$, $\rho_0=0.001$, $\gamma_0=0.01$, $\epsilon_0=0.01$, $\lambda_0=0.01$, $\nu_0=0.0001$.

E.4. Training-data poisoning

For this experiment, we used l_2 -regularized logistic regression implemented as a single layer neural network with the cross entropy loss and a weight regularization term with a coefficient of 0.05. The model is trained for 10000 epochs using the Adam optimizer with learning rate of 0.001 for training with and without poisoned data. We pre-train the

lower-level with clean training data for 5000 epochs with the Adam optimizer and learning rate 0.001 before starting bilevel training. For untargeted attacks, we optimized Penalty with $K = 5000$, $T = 20$, $\sigma_0=0.1$, $\rho_0 = 0.001$, $\gamma_0=10$, $\epsilon_0=1$, $\lambda_0=100$, $\nu_0=0.0$. The test accuracy of this model trained on clean data is 87%. For targeted attack, Penalty is optimized with $K = 5000$, $T = 20$, $\sigma_0=0.1$, $\rho_0 = 0.001$, $\gamma_0=10$, $\epsilon_0=1$, $\lambda_0=1$, $\nu_0=0.0$.

E.4.1. CLEAN LABEL ATTACK

The goal of clean label attack is to find poisoning points which appear to have correct labels, when visually inspected, but a classifier trained on original training data augmented with these poisoned points, leads to misclassification of specific target images. We use the dog vs. fish image dataset as used by [Koh & Liang, 2017], consisting of 900 training and 300 testing examples from each of the two classes. The size of the images in the dataset is 299×299 with pixel values scaled between -1 and 1. Following the setting in Sec. 5.2 of [Koh & Liang, 2017], we use InceptionV3 network, with weights pre-trained on ImageNet, for our representation map (2048 dimensional) and train a fully connected layer on top of this representation to classify dogs and fishes. For a given target image t from the test set, a base image b whose representation is the closest to the representation of the target image and has the opposite label is chosen from the training set. Inspired by [Shafahi et al., 2018], we use the following bilevel formulation:

$$\begin{aligned} \arg \min_u L_t(u, w) + \alpha \|r(t) - r(u)\|_2^2 + \beta \|b - u\|_2^2 \\ \text{s.t. } w = \arg \min_w L_{X \cup \{u\}}(w), \end{aligned} \quad (10)$$

where L_t is the loss of the given target image associated with the opposite label, and $r(\cdot)$ is the 2048-dimensional representation obtained from the InceptionV3 model. The second term in the upper-level penalizes the difference between the representations of the poisoned image and the target image t , and the third term in the upper-level forces the poisoned image to be close to the base image b in the input space ensuring that the poisoned image appears similar to the base image to avert detection. α and β control the relative importance of these terms. To test the performance of the attack we retrain only the fully connected layer with original training data augmented with the poisoned point obtained from Penalty. Attack is considered successful if the target point, which is correctly classified before poisoning (there are 590 such test images out of 600), is misclassified after retraining on the augmented training dataset. We generate poisoned point for each target image one by one. The attack success of Penalty using just a single poisoned point per target image is 100%. Attack success with using a single poisoned point by [Koh & Liang, 2017] and [Shafahi et al., 2018] are 57% and 100% respectively. As shown in Fig. 7,



Figure 5. Untargeted data poisoning attack on MNIST. Top row shows the learned poisoned image using Penalty, starting from the images in the bottom row as initial poisoned images. The column number represents the fixed label of the image, i.e. the label of the images in first column is digit 0, second column is digit 1, etc.



Figure 6. Targeted data poisoning attack on MNIST. Top row shows the learned poisoned images using Penalty, starting from the images in the bottom row as initial poisoned images. Images in the first 5 columns have the fixed label of digit 3, and in the next 5 columns are images with the fixed label of digit 8.

poisoned points obtained by solving Eq. (10) are indistinguishable from the original base points but still misclassify the target point during retraining.

Experiment Details: We use the InceptionV3 model with weights pre-trained on ImageNet. We train a dense layer on top of these pre-trained features using the RMSProp optimizer and a learning rate of 0.001 optimized for 2000 epochs. Test accuracy obtained with training on clean training data is 98.33. We repeat the exact same procedure as training during evaluation and train the dense layer with training data augmented with poisoned point obtained from Penalty. Penalty is optimized with $K = 600$, $T = 10$, $\sigma_0=0.01$, $\rho_0 = 0.001$, $\gamma_0=1$, $\epsilon_0=1$, $\lambda_0=1$.



Figure 7. Clean label poisoning attack on dog-fish dataset. The top row shows the target instances from the test set, the second row shows the base instances from the training set used to initialize the poisoned images and the last row shows the poisoned instances obtained from Penalty. Notice that poisoned images (third row) are visually indistinguishable from the base images (second row) and can evade visual detection.